Journal Pre-proofs

Anaerobic consortia mediate Mn(IV)-dependent anaerobic oxidation of methane

Wenbo Liu, Sai Xu, Hongpu Ma, Yuanyuan Li, Jacek Mąkinia, Jun Zhai

PII: S1385-8947(23)02209-X
DOI: https://doi.org/10.1016/j.cej.2023.143478
Reference: CEJ 143478

To appear in: *Chemical Engineering Journal*

Received Date: 17 February 2023
Revised Date: 13 April 2023
Accepted Date: 9 May 2023

Please cite this article as: W. Liu, S. Xu, H. Ma, Y. Li, J. Mąkinia, J. Zhai, Anaerobic consortia mediate Mn(IV)-dependent anaerobic oxidation of methane, *Chemical Engineering Journal* (2023), doi: https://doi.org/10.1016/j.cej.2023.143478

Anaerobic consortia mediate Mn(IV)-dependent anaerobic oxidation of methane

Wenbo Liu [1,2], Sai Xu[3], Hongpu Ma [1], Yuanyuan Li [1], Jacek Mąkinia [4], Jun Zhai [1,2 *]

Affiliations

[1] College of Environment and Ecology, Chongqing University, Chongqing, 400045, China

[2] Institute for Smart City of Chongqing University in Liyang, Chongqing University, Jiangsu, 213300, China

[3] School of Environmental and Biological Engineering, Nanjing University of Science and Technology, Nanjing, 210094, China

[4] Faculty of Civil and Environmental Engineering, Gdansk University of Technology, 80-233, Gdańsk, Poland

*Corresponding author. E-mail: zhaijun@cqu.edu.cn (J.Z.)

Abstract

Manganese-dependent anaerobic oxidation of methane (Mn-AOM) is a major methane sink and vital to mitigating global warming. However, it is difficult for microorganisms to mediate electron transfer between the hardly dissolved CH_4 and insoluble Mn(IV) minerals, leading to poor understanding of species mediating Mn-AOM. This study successfully enriched an anaerobic consortium mediating AOM driven by Mn-dependent respiratory growth, and for the first time, revealing a syntrophic pathway for Mn-AOM. The Mn-AOM occurrence was confirmed by long-term bioreactor performance and ^{13}C-labelling batch experiment. Metagenomic and metatranscriptomic analyses demonstrated that the *Candidatus Methanoperedens* sp. BLZ1 was responsible for CH_4 oxidation. The *Luteitalea pratensis* mediated extracellular electron transfer crossing S-layer of *Ca. M.* BLZ1 by conductive pili, and mediated microbial Mn(IV) reduction via multi-heme *c*-type cytochromes. This study offers an alternative syntrophic pathway for Mn-AOM by a microbial consortium instead of previously reported pathway by ANME alone. These outcomes provided new insight into migrating global climate change and manganese cycles.

Keywords: Anaerobic oxidation of methane; manganese; multi-heme *c*-type cytochromes; extracellular electron transfer

1. Introduction

Methane (CH_4) is the second most important greenhouse gas after carbon dioxide (CO_2) [1], with the global warming potential 28 times higher than CO_2 [1]. Anaerobic oxidation of methane (AOM), coupled with reduction of nitrate and nitrite [2, 3], sulfate [4, 5], metal oxides [6, 7], humic acids [8], and biochar [9], is important to regulate global CH_4 emission [10]. The Mn(IV)- and Fe(III)-bearing minerals are widely distributed in the biosphere. They are also thermodynamically favourable and biochemically feasible electron acceptors for AOM. The Mn(IV)- and Fe(III)-dependent AOM (Mn-AOM and Fe-AOM) has been observed in in marine [7] and freshwater sediments [11]. They both are major global CH_4 sinks and considered as vital energy sources for the early Earth [6]. However, the growth of species mediating Mn-AOM is slow and poorly explored. This is attributed to the difficulty of electron transfer between the hardly dissolved CH_4 and insoluble Mn(IV). Up to now, only two ANMEs (anaerobic methanotrophic archaea) were enriched from AOM mediated by Mn-dependent respiratory growth, namely *Candidatus Methanoperedens manganicus* and *Candidatus Methanoperedens manganireducens* [12]. These species can perform Mn-AOM independently via extracellular electron transfer and microbial Mn(IV) reduction. In the extracellular electron transfer, both two ANMEs can use the multi-heme *c*-type cytochromes (MHCs) to bridge the nonconductive S-layer by forming MHC/S-layer fusion protein [12]. Then, these ANMEs make contact with the minerals for Mn(IV) reduction, with a certain amino acid motif at the C-terminus of the MHC protein ([ST]-[AVILMFYW]-[ST]-P-[ST]) [13, 14].

Some ANMEs can use Mn(IV) as alternative electron acceptor mediating AOM. The *Candidatus Methanoperedens* sp. BLZ1 (formerly known as *Methanoperedens nitroreducens* MPEBLZ), cultured under anaerobic, nitrate-reducing conditions, is able to mediate Mn(IV)-AOM[15]. However, the *Ca. M.* BLZ1 lacks the proteins for crossing the archaeal S-layer. It is still mysterious for extracellular electron transfer of *Ca. M.* BLZ1[16]. Besides, this species also lacks the specific mineral-binding motifsfor electron transfer between microorganism and insoluble Mn(IV) minerals [16]. Further studies are needed to reveal the mechanisms for Mn-AOM mediating by *Ca. M.* BLZ1.

This study aimed to enrich and characterize the Mn-dependent respiratory microorganisms that can perform AOM. The microbial process was determined through mass and electron balance and isotopic tests. Microorganisms involved in Mn-AOM were identified and characterized through metagenomic and metatranscriptomic analyses. These results increase the understanding of Mn-AOM and its role in global methane and Mn cycling. Moreover, the results can also provide new insight into the mitigation of global warming and climate change.

2. Methods and Materials

2.1 Bioreactor setup and operation

A 2.5 L sequencing batch reactor (SBR) was operated for over 820 days to enrich the microorganisms mediating the Mn-AOM process (Fig.S1). The culture was collected from a lab-scale constructed wetland filled with natural Mn ores (Text S1) [17]. In total, a 1.7 L mixture of culture and synthetic medium (Text S2) was filled, leaving 0.8 L headspace. Every 30 days, about 500 mL supernatant of the bioreactor

was replaced by the newly synthesized medium.

Meanwhile, synthetic δ-MnO_2 slurry (stock solution at 4 gMn/L), prepared according to the modified Murry's method (Text S3) [17], was added as the sole electron acceptor. Subsequently, the reactor was bubbled with pure N_2 for maintain anaerobic conditions. During the entire experiment, the O_2 in the headspace was consistently below the detection limit (< 0.002% v/v). Next, the CH_4 (99.999%) was supplied as the sole electron donor by flushing the liquid and headspace for 10 min. The reactor was operated at 30 ± 2 °C in a thermostatic water cabinet in the dark, and was mixed gently with a magnetic stirrer at 150 rpm. The pH was maintained at ~7.0 by dosing 1 M HCl.

Generally, liquid samples were withdrawn regularly (Text S4). After extraction and filtration, the samples were used to measure the final products of Mn-AOM, including generated Mn(II), soluble Mn(III), dissolved CO_2, and precipitated carbonate. The gas samples were also withdrawn for chemical analysis of CH_4 and CO_2, performed as described previously [17] (see in Text S4).

2.2 Isotopic labeling and stoichiometry test

On day 820, the reactor was refreshed by the new medium, including δ-MnO_2 and CH_4. After that, about 150 mL $^{13}CH_4$ (Sigma-Aldrich, 99 atom % ^{13}C, USA) was manually injected into the reactor. Every three days, gas samples were withdrawn from the headspace to measure CH_4 and CO_2, and $^{13}CO_2$. The mixed liquid and solid samples were withdrawn simultaneously to detect the $\delta^{13}C$, Mn(II) and Mn(IV) (see in Text S4). The $\delta^{13}C$ stable isotopic ratio of CO_2 was measured with a stable isotope ratio mass spectrometer (isoprime precisION, Elementar, Germany).

The stoichiometry test was performed by using a subsample of bioreactor biomass in duplicate. In total, 300 mL subsamples were transferred anaerobically to a 500 mL of a glass vessel. Every 3 days, gas samples were withdrawn from the headspace for measurement of CH_4 and CO_2 and the Mn(II) concentration in the liquid. The consumption rate of CH_4 (rCH_4) and the production rate of Mn(II) (rMn(II), representing the consumption of Mn(IV)) were calculated via linear regression. The quantitative ratio between rCH_4 and rMn(II) was calculated for the stoichiometry test.

2.3 Metagenomic and metatranscriptomic analysis

(1) Metagenomic analysis. Sample collected from the bioreactor on day 820 was used for metagenomic analysis. A paired-end library was prepared using the TruSeq PE Cluster Kit v3-cBot-HS and TruSeq SBS Kit v3-HS (Illumina, USA). The library was sequenced on the HiSeq 2000 (Illumina) platform.

Paired-end reads for the initial metagenome were trimmed using Seqprep (https://github.com/jstjohn/SeqPrep) and Sickle v1.33 (https://github.com/najoshi/sickle) using the default settings. The reads were assembled using IDBA-UD [19] (http://i.cs.hku.hk/~alse/hkubrg/projects/idba_ud/), a de novo assembler. The resulting assembly consisted of 676561 contigs ≥ 300 bp with an N50 of 1470 bp, and a total of ~ 691 Mbp of sequence data.

Population genomes were recovered from the assembled contigs and unmapped reads using MetaBat (https://bitbucket.org/berkeleylab/metabat, v2.12.1) [20].

Therecovered draft genomes were further treated by refineM (https://github.com/dparks1134/RefineM) and dRep (https://github.com/MrOlm/drep) [21]. Completeness and contamination of the population bins were assessed using CheckM [22].

The annotation of assembled contigs for taxonomy was used AMPHORA2 (https://github.com/martinwu/AMPHORA2), while the functional annotation was used BLASTP (BLAST Version 2.2.31+, http://blast.ncbi.nlm.nih.gov/Blast.cgi) against protein family databases (Pfam, COG, and KEGG).

(2) Metatranscriptomic analysis. The metatranscriptomic paired-end reads were quality trimmed using bmtagger with the default settings and the contig was obtained by using Trinity. Subsequently, the assembled contigs used TransGeneScan for gene annotation and MMseqs2 for protein annotation. The soap.coverage (https://github.com/aquaskyline/SOAPcoverage) was used to determine the counts for the contigs, and the RNA-TPM was calculated the same as described in other studies [12].

2.4 Visualization of Mn-AOM microbial aggregates by transmission electron microscopy (TEM)

The fluorescence in situ hybridization (FISH) analysis was performed as described by Ettwig et al. [23] to locate the ANME-2d (Cy-3(red) labeled AAA-641 probe [24]), other archaea (FITC (green) dye-labeled Arch-0915 probe) and bacterial species (DAPI, blue) potentially involving Mn-AOM (Text S5). Then the sample were used to examine by the TEM.

The TEM analysis was performed based on a modified protocol described in the previous studies [25]. The samples examined by FISH analysis were embedded into LR white by a graded ethanol series (15 minutes each of 25%, 50%, 75%, 100% × 3 times). Subsequently, the samples were embedded by 50% LR White Resin and 50% ethanol for 30 min on a shaker at room temperature and then moved to 100% LR White Resin for 1 hour. The polymerization was conducted for 48 h at 56°C. The target areas marked by FISH were taken from the slides and transferred into a tube containing 5% phosphotungstic acid hydrate in 100mM HEPES (pH 7.8) and then incubated 90 min on ice. The samples were embedded again as described above (see in Fig.S2). The block was then sectioned at 200nm and examined using a FEI Talos F200S transmission electron microscope (ThermoFisher Scientific Co., USA).

3. Results and Discussion

3.1 Observation of Mn(IV)-dependent AOM in the laboratory-scale sequencing batch reactor (SBR)

A laboratory-scale sequencing batch reactor (SBR) was performed for about 820 days to enrich microorganisms mediating Mn-AOM. The inoculum, from a constructed wetland filled with natural Mn ores [17], was fed with CH_4 and δ-MnO_2 as the sole electron donor and electron acceptor, respectively. After 200-day pre-cultivation, stable CH_4 oxidation was observed (Fig. 1a). The observed stoichiometric ratio of r[Mn(IV)]/r[CH_4] (ratio between Mn(IV) reduction rate and CH_4 consumption rate) was 4.01:1, while that of r[Mn(II)]/r[CH_4] (ratio between Mn(II) generation rate and CH_4

consumption rate) was 3.83:1 (Fig.1b). Both values are close to the theoretical stoichiometric ratio of 4:1 for Mn-AOM (Table S1). Other soluble electron acceptors were found at low concentrations in the SBR (NO_3^-, <20μg/L; NO_2^-, <10μg/L; SO_4^{2-}, 4.36 mg/L; Fe(III), 0.05mg/L, Table S2). Therefore, the AOM occurred in the bioreactor was mainly coupled with Mn(IV) reduction, namely Mn-dependent AOM. The final product of CH_4 oxidation was CO_2, remaining as carbonate in the solid and liquid phases as reported [12] (Fig.1c). As a result, the CH_4 consumption rate is higher than the CO_2 production rate in the bioreactor's headspace. The observed microbial CH_4 oxidation rate (0.6 pmol/d/cell) was comparable with the reported Mn-AOM [12] (Table 1).

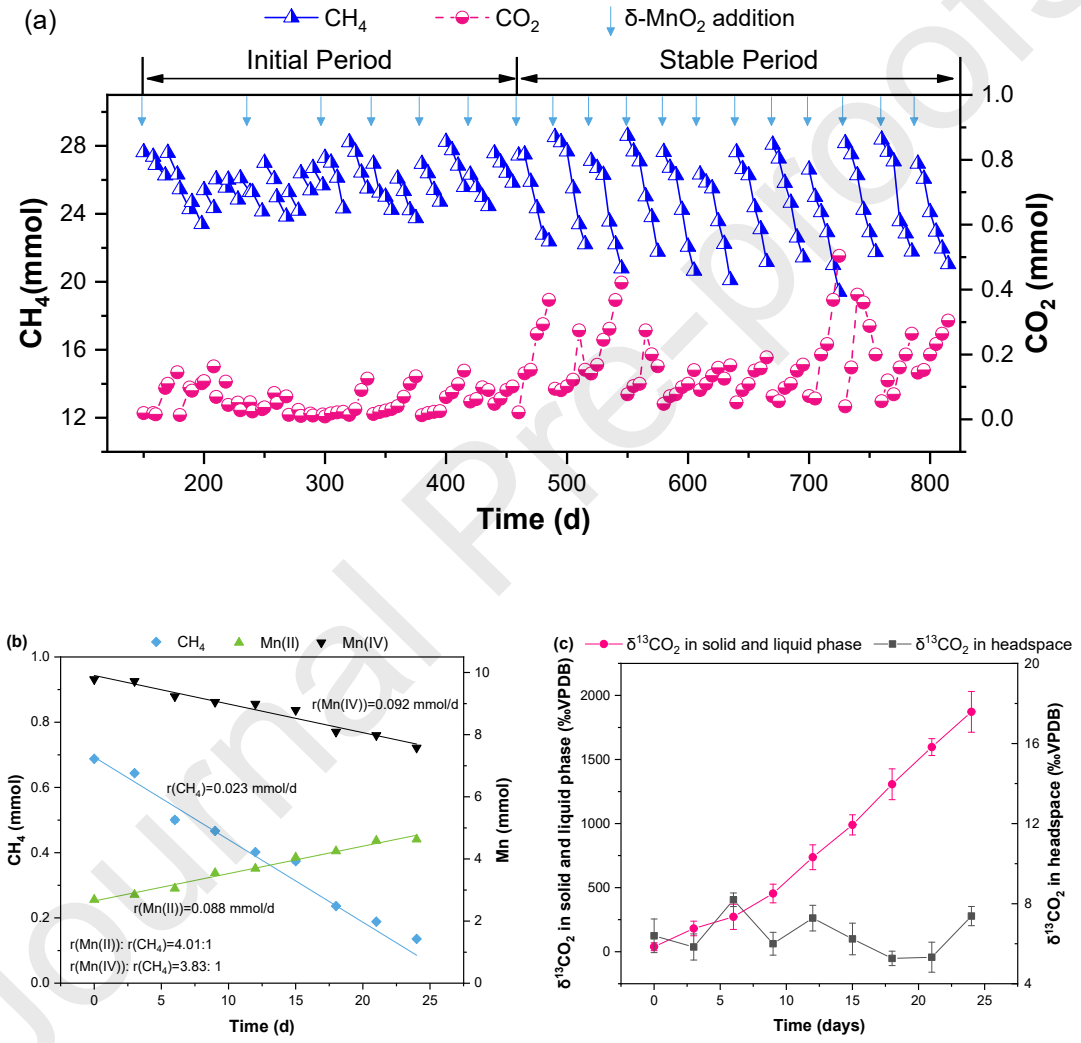

Fig. 1. Performance of the laboratory-scale sequencing batch reactor and batch experiments. (a) Total CH_4 reduction and total CO_2 production during the long-term cultivation. The blue arrows indicate δ-MnO_2 additions (the continuing cultivation in Fig.S1); (b) The profiles of Mn(II) and CH_4 during the stoichiometry (batch) test on day 820; (c) Conversion of $^{13}CH_4$ during the isotopic (batch) test on day 820. The error bars stand for standard deviation of replicated bottles (n=3).

Table 1. Observed CH_4 consumption rates in anaerobic oxidation of methane (AOM) coupled with reduction of Mn.

Key microorganisms for AOM	Observed microbial CH_4 consumption rate (pmol/d/cell)	Reference
Ca. M. manganicus *Ca. M. manganireducens*	0.4 - 0.5	[12]
ANME-2d lineage	0.6	[17]
Ca. M. BLZ1	0.3×10^{-3}	[15]
Ca. M. BLZ1	0.2 (initial period, day 150-460) 0.6 (stable period, day 460-820)	This study

3.2 Genome recovery and microbial community analysis

The metatranscriptomic analysis showed high expression of *mcr*A gene (methyl-coenzyme M reductase alpha subunit gene, TPM=2211.39), which was the key gene in "reverse methanogenesis" pathway [26] and thus proved this pathway was the primary CH_4 oxidation process in this study (Fig.2). The particulate methane monooxygenase (*pmo*) genes, both for *Methylomirabilis oxyfera* (NC10 phylum) mediating nitrite-AOM via intracellular O_2 production [3, 27] and for aerobic methane oxidation [28], were hardly expressed (TPM=70.20). Besides, the O_2 content in the bioreactor's headspace was extremely low (< 0.002%, v/v). Therefore, the possibility of aerobic methane oxidation pathway and nitrite-dependent AOM pathway by *M. oxyfera* were excluded.

The metagenomic analysis revealed that an archaeon containing genes encoded complete "reverse methanogenesis" (Fig.2) was enriched (from 1.4% to 96.3% in the archaeal community), and finally accounting for 6.6% of the whole microbial community (Fig.S2). This archaeon was proven to be *Ca. M.* BLZ1 by comparative analysis (Table S4, S5), with the average amino acid identity (AAI) of 97.7% and average nucleotide identity (ANI) of 98.1% (Text S6, Table S4, S5). Besides, the CH_4

oxidation rate had a linear relationship with the number of *Ca. M.* BLZ1 (R^2=0.94). In addition to "reverse methanogenesis", the *Ca. M.* BLZ1 also contained genes encoding enzymes catalyzed for multiple energy conversion and intracellular electron transfer, including heterodisulfide reductase (*hdr*), Na^+ translocating methyltransferases (*Mtr*), coenzyme B, ferredoxin, and Cofactor F_{420} (Fig. 2b, Fig.4).

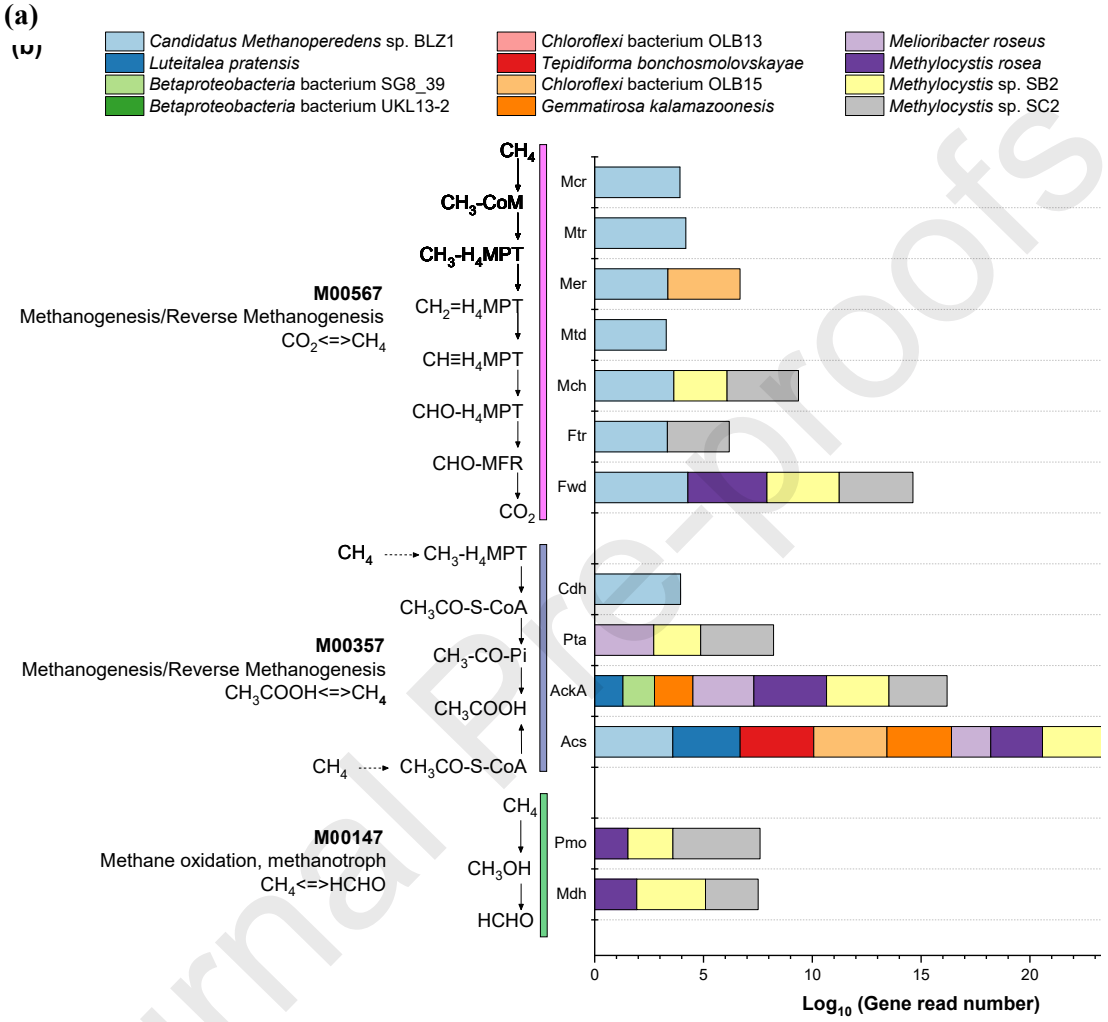

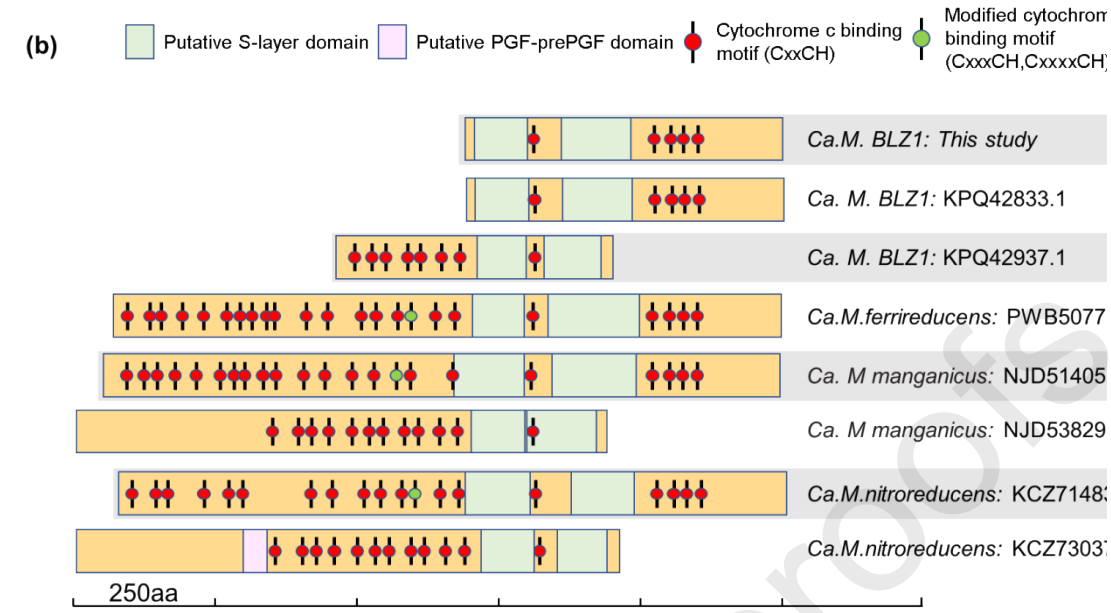

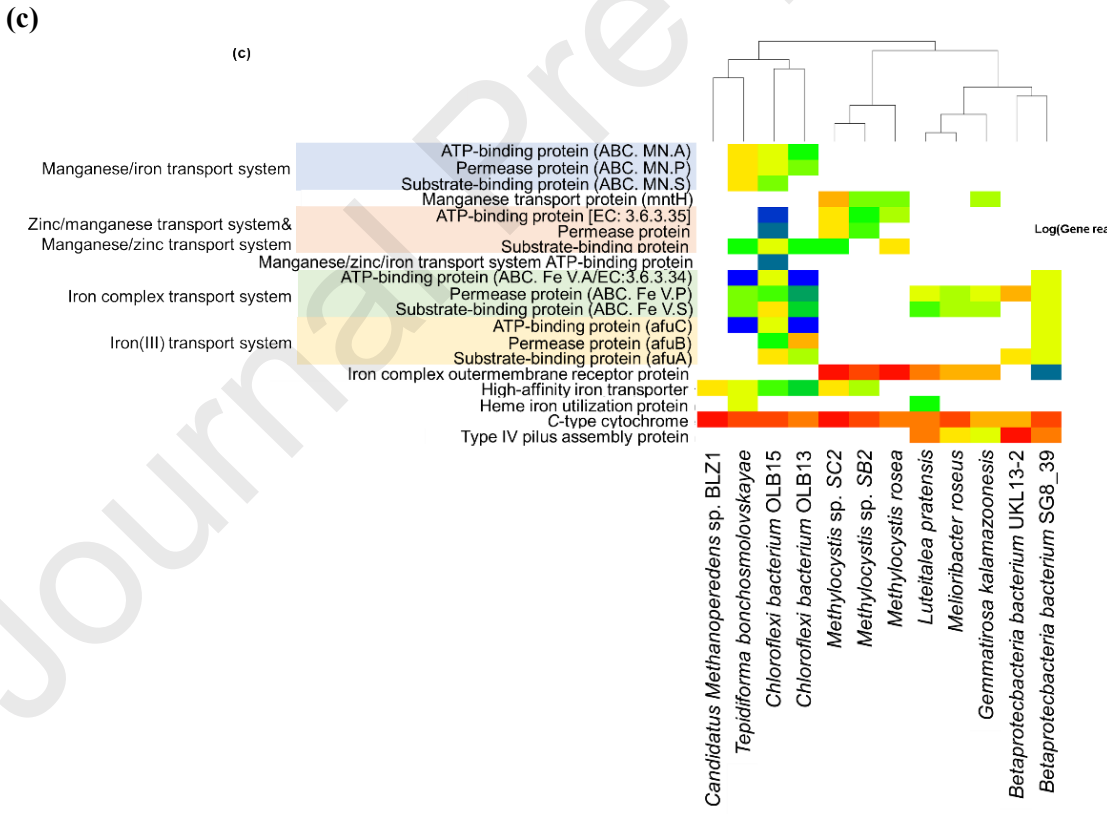

192 **Fig. 2. Metagenomic analysis of the microbial consortia in the bioreactor.** (a) Reads
193 number of the key genes encoded CH_4 metabolism pathway; (b) Multi-heme c-type
194 cytochrome with predicted S-layer domains from the reconstructed genomes. Protein
195 schematics are simply positioned to show compositional similarity, not a sequence

alignment. Each vertical tick-mark denotes 250 amino acids. The gene identifier numbers are shown on the right; (c) Heatmap of genes (reads number) encoded enzymes possibly involving electron transfer and Mn(IV) reduction.

However, *Ca. M.* BLZ1 could not mediate Mn-AOM independently because it lacked proteins for extracellular electron transfer crossing the archaeal S-layer, which was non-conductive and non-penetrative [29], and also lacked the specific binding motifs for electron transfer to insoluble Mn(IV) minerals. Therefore, archaea or bacteria capable of transferring electrons to insoluble Mn(IV) and mediating microbial Mn(IV) reduction, were expected to be the consortia microbial partner. In the archaeal community, the proportion of other archaea was less than 0.1%. It was unlikely that the archaea with small proportions could mediate extracellular electron transfer for Mn(IV) reduction.

The *L. pratensis* (1.71% of total microbial community), rather than widely reported metal-reducing bacteria (*Shewanella*, 0.007% of the community; *Geobacter*, not found in our bioreactor), was the bacterial partner in Mn-AOM in the SBR. The *L. pratensis* contained genes encoding MHCs for extracellular electron transfer and metal reduction [30, 31], and the MHCs contained the specific amino acid sequence for Mn(IV)-mineral binding.

Instead of enriching *Ca. M. manganicus* and *Ca. M. manganireducens*, *Ca. M.* BLZ1 was successfully enriched in our bioreactor with continuous long-term incubation. This microorganism was earlier enriched through nitrate/nitrite-AOM [16], but the low concentrations of NO_3^- (< 20μg/L) and NO_2^- (<10μg/L) excluded their contribution to AOM in this study. In the Mn-AOM, microbial Mn(IV) reduction was performed via two one-electron transfer steps [32], and Mn(III) was the intermediate. The generated Mn(III) will be reduced immediately to Mn(II) by the metal reductase on the surface of bacteria , or rapidly converted into Mn(II) and Mn(IV) via disproportionation [33], leading no Mn^{3+} detected in our bioreactor via spectrophotometric method (absorbance at 258 nm of Mn(III) complex with pyrophosphate) [33]. It is a coincidence that the *Ca. M.* BLZ1 was enriched both from nitrate-AOM and Mn-AOM cultures, indicating there were some specific ecological niches that respiratory growth of *Ca. M.* BLZ1 in both cultures, but requiring further investigation.

3.3 Extracellular electron transfer between *Ca. M.* BLZ1 and *L. pratensis*

The *Ca. M.* BLZ1 cannot perform extracellular electron transfer across the S-layer, because its genes encoded MHC/S-layer fusion protein incapable of forming complete "bridge" crossing the S-layer (Fig.2c), and it has no genes encoded conductive archaellum(archaeal conductive nanowire). On the contrary, the *Ca. M. manganicus* contained MHC/S-layer proteins possessing 12 and 22 hemes, while *Ca. M.manganireducens* contained MHC/S-layer proteins processing 113, 52 and 19 hemes [12]. Besides, the *Ca. M. manganicus* can also use conductive archaellum for electron transfer in Mn-AOM [12].

The *Ca. M.* BLZ1 contains no genes for formate formation, H_2 production, or

membrane-bound H_2-uptake NiFe hydrogenases. Besides, no formate in liquid or H_2 in the headspace was detected in our bioreactor (Table S2). The genes encoding the enzymes for the complete acetoclastic methanogenesis pathway were found in *Ca. M.* BLZ1 [16], but the key genes of acetyl-CoA decarbonylase/synthase (*cdh*) were not expressed, and expression of acetyl-CoA synthetase (*ACS*) was low (TPM=41.1). Besides, the acetate was not found in the water stream. No microorganisms in our bioreactor contained genes encoding the complete dissimilatory sulfate reduction, resulting in that the novel Mn(IV)-supported sulfate-AOM [34], using Mn(IV) to oxidize sulfur species from sulfate-AOM, was excluded in our bioreactor.

The conductive pili were shown by the TEM image (Fig.3, in red circle). The conductive pili connected the *Ca. M.* BLZ1 (spherical shape) and *L. pratensis* (rod-shaped), mediating extracellular electron transfer (Fig.3a,c). Besides, the direct contact between *L. pratensis* and Mn(IV)-minerals was observed (Fig.3), which was also suitable for extracellular electron transfer in Mn(IV) reduction [35].

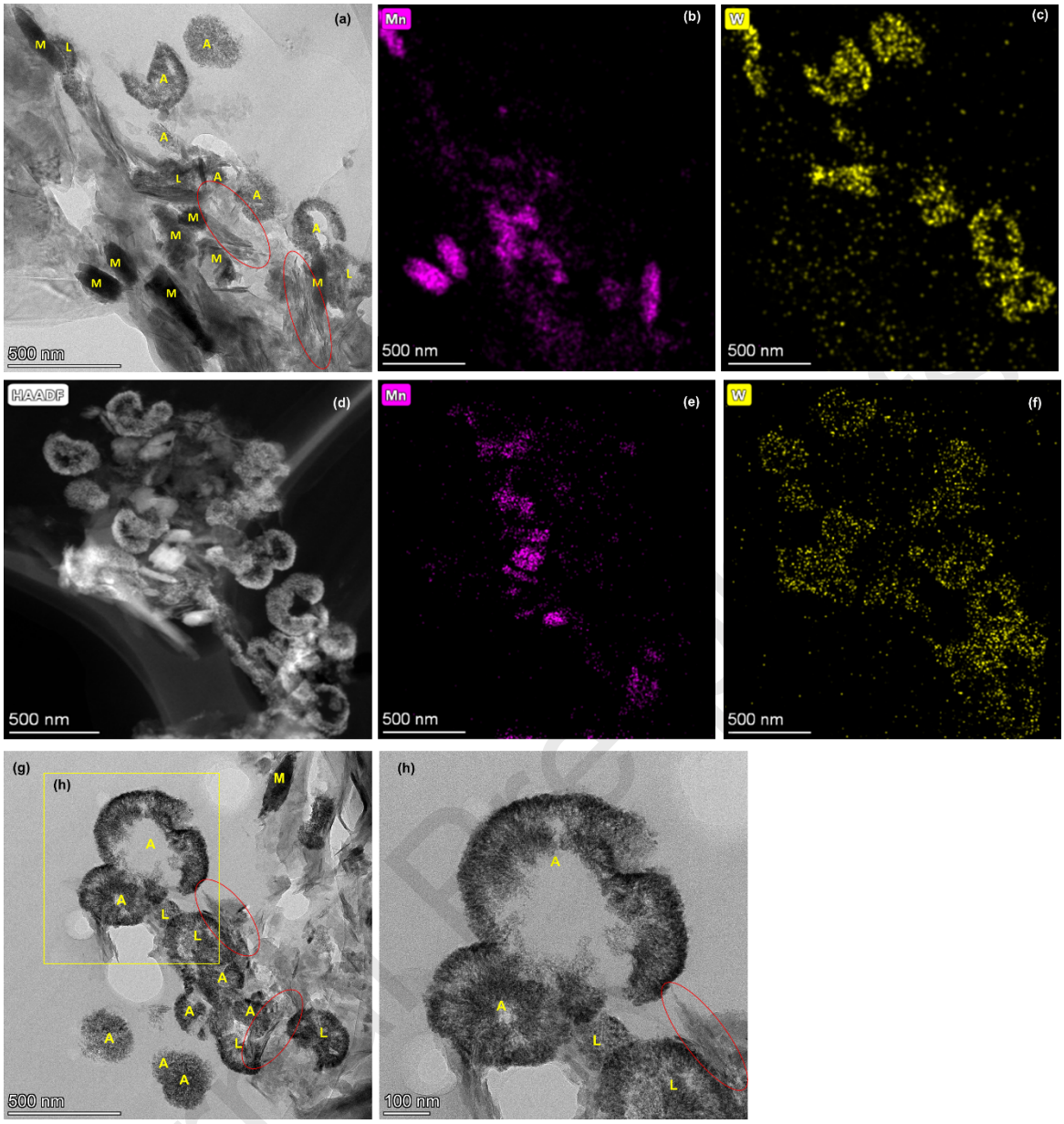

Fig. 3. Spatial location of microbial consortia mediating Mn-AOM in our bioreactor. A: *Candidatus Methanoperedens* sp. BLZ1 (spherical shape); B: *Luteitalea pratensis* (rod-shaped [31]); M: δ-MnO_2. The conductive nanowire structure was marked in the red circle. The scale was listed in the picture. (a), (d), (g) and (h) were the TEM image; (b) and (e) the image of element Mn by TEM; (c) and (f) the image of element W by TEM (representing for microorganisms).

In our bioreactor, *L. pratensis* encoded conductive pili (Fig. 2c), assist the electron crossing the S-layer of the *Ca. M.* BLZ1. Then, these electrons were transported through the MHCs containing in the *L. pratensis* and finally to terminal electron acceptor (Mn(IV)-minerals). (Fig.4). The MHCs, including OmcS, MtrC and OmcA, was highly expressed (TMP= 1240.63). Both MtrC and OmcA were metal reductase [36, 37] while the OmcS could form the specific bond with the mineral surface [38]. These MHCs participated in microbial Mn(IV) reduction by direct transfer of the electrons to

insoluble MnO_2.

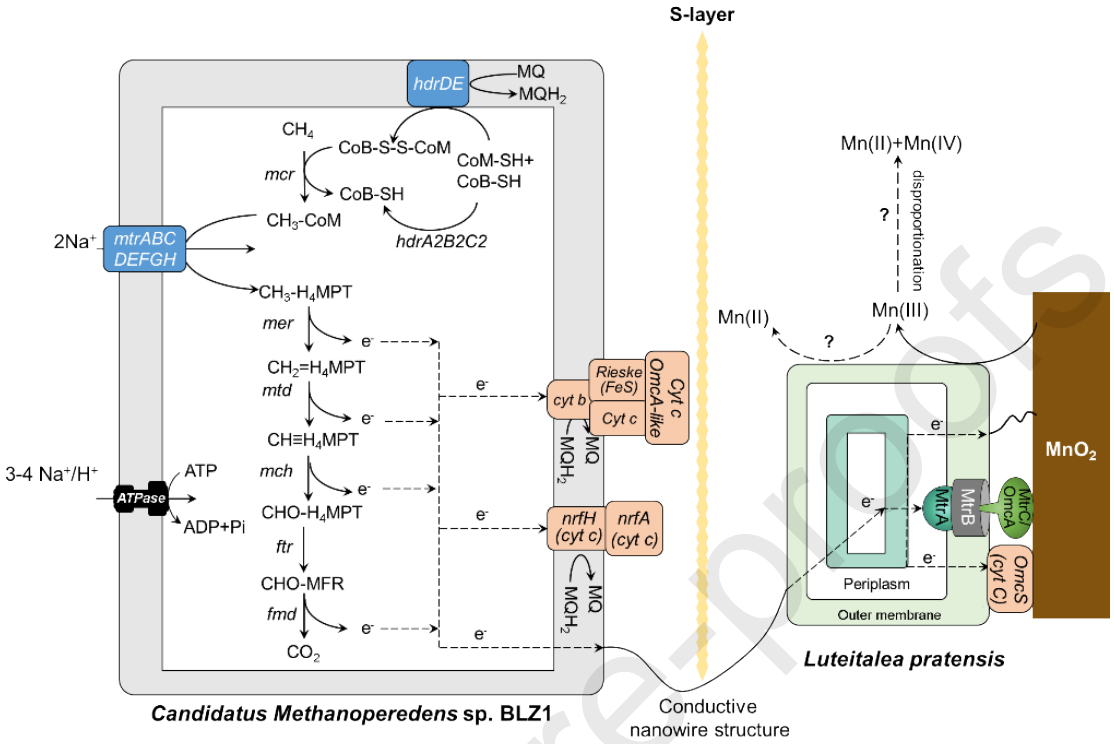

Fig. 4. Putative syntrophic pathway for Mn-AOM by *Candidatus Methanoperedens* sp. BLZ1 and *Luteitalea pratensis*. Abbreviations for enzymes and co-factors: *mcr*, methyl-coenzyme M reductase; *mtr*, Na^+-translocating methyl-H_4MPT:coenzyme M methyltransferase; *mer*, F_{420}-dependent methylene-H_4MPT reductase; *mtd*, F_{420}-dependent methylene H_4MPT dehydrogenase; *mch*, methenyl-H_4MPT cyclohydrolase; *ftr*, formylmethanofuran–H_4MPT formyltransferase; *fmd*, formyl-methanofuran dehydrogenase (also known as *fwd*); *frh*, F_{420}-reducing hydrogenase; *hdr*, heterodisulfide reductase; *nrf*, cytochrome c nitrite reductase; *cyt*b, b-type cytochrome; *cyt*c, c-type cytochrome; FeS, ferredoxin iron sulfur protein; MtrABC, metal-reducing outer membrane decahaem cytochrome c; CoB-SH, coenzyme B; CoM-SH, coenzyme M; CoB-S-S-CoM, Coenzyme M-HTP heterodisulfide; H_4MPT, tetrahydromethanopterin; Fd, ferredoxin; MQ, menaquinone; MQH_2, menaquinol.

4. Conclusion

In conclusion, unlike previously reported Mn-AOM mediated by ANME alone, this study revealed a syntrophic pathway by an anaerobic consortium. In this consortium, *Ca. M.* BLZ1 encoded and expressed genes for the "reverse methanogenesis", converting CH_4 to CO_2. The *L. pratensis*, as a bacterial partner, assisted the extracellular electron transfer from archaea to terminal Mn(IV) minerals and microbial Mn(IV) reduction. The electrons generated from CH_4 oxidation acrossed

the archaeal S-layer via the conductive pili of *L. pratensis*. Then, those electrons were used for Mn(IV) reduction through MHCs, including metal reductases like MtrA and OmcA, and OmcS. This study expands the knowledge and provides new insight into the metabolic characteristics of *Methanoperedenaceae* family and Mn(IV)-AOM. The syntrophic pathway for Mn-AOM is vital for migtagating the global climate change and manganese cycles.

Acknowledgments

This research was financially supported by the National Natural Science Foundation of China (No. 51878093) and National Natural Science Foundation of China for Young Scientist of China (No. 52000015). The microbial analysis, metagenomics, assembling, binning and annotation were performed by Major Bio (Shanghai, China). The metatranscriptomic analysis was performed by Personalbio (Shanghai, China).

References

[1] IPCC, Climate Change 2021: The Physical Science Basis, in: I.T.c.w. team (Ed.), IPCC, 2021.

[2] M.F. Haroon, S.H. Hu, Y. Shi, M. Imelfort, J. Keller, P. Hugenholtz, Z.G. Yuan, G.W. Tyson, Anaerobic oxidation of methane coupled to nitrate reduction in a novel archaeal lineage, Nature 500 (2013) 567-570.

[3] K.F. Ettwig, M.K. Butler, D. Le Paslier, E. Pelletier, S. Mangenot, M.M. Kuypers, F. Schreiber, B.E. Dutilh, J. Zedelius, D. de Beer, J. Gloerich, H.J. Wessels, T. van Alen, F. Luesken, M.L. Wu, K.T. van de Pas-Schoonen, H.J. Op den Camp, E.M. Janssen-Megens, K.J. Francoijs, H. Stunnenberg, J. Weissenbach, M.S. Jetten, M. Strous, Nitrite-driven anaerobic methane oxidation by oxygenic bacteria, Nature 464 (2010) 543-548.

[4] S. Scheller, H. Yu, G.L. Chadwick, S.E. McGlynn, V.J. Orphan, Artificial electron acceptors decouple archaeal methane oxidation from sulfate reduction, Science 351 (2016) 703-707.

[5] E. Bell, T. Lamminmäki, J. Alneberg, C. Qian, W. Xiong, R.L. Hettich, M. Frutschi, R. Bernier-Latmani, Active anaerobic methane oxidation and sulfur disproportionation in the deep terrestrial subsurface, Isme J 16 (2022) 1583-1593.

[6] O.E. Oni, M.W. Friedrich, Metal oxide reduction linked to anaerobic methane oxidation, Trends Microbiol 25 (2017) 88-90.

[7] E.J. Beal, C.H. House, V.J. Orphan, Manganese- and iron-dependent marine methane oxidation, Science 325 (2009) 184-187.

[8] Y.N. Bai, X.N. Wang, J. Wu, Y.Z. Lu, L. Fu, F. Zhang, T.C. Lau, R.J. Zeng, Humic substances as electron acceptors for anaerobic oxidation of methane driven by ANME-2d, Water Res 164 (2019) 114935.

[9] X. Zhang, J. Xia, J. Pu, C. Cai, G.W. Tyson, Z. Yuan, S. Hu, Biochar-mediated anaerobic oxidation of methane, Environ Sci Technol 53 (2019) 6660-6668.

[10] C.-H. Cheng, S.A.T. Redfern, Impact of interannual and multidecadal trends on methane-climate feedbacks and sensitivity, Nat Commun 13 (2022) 3592.

[11] W.-X. Hu, X. Kang, J. Cao, X.-L. Wang, B. Fu, H.-G. Wu, Thermochemical oxidation of methane induced by high-valence metal oxides in a sedimentary basin, Nat Commun 9 (2018) 5131.

[12] A.O. Leu, C. Cai, S.J. McIlroy, G. Southam, V.J. Orphan, Z.G. Yuan, S.H. Hu, G.W. Tyson, Anaerobic methane oxidation coupled to manganese reduction by members of the *Methanoperedenaceae*, Isme J 14 (2020) 1030-1041.

[13] A.V. Mardanov, G.B. Slododkina, A.I. Slobodkin, A.V. Beletsky, S.N. Gavrilov, I.V. Kublanov, E.A. Bonch-Osmolovskaya, K.G. Skryabin, N.V. Ravin, The *Geoglobus acetivorans* genome: Fe(III) reduction, acetate utilization, autotrophic growth, and degradation of aromatic compounds in a hyperthermophilic archaeon, Appl

Environ Microb 81 (2015) 1003-1012.

[14] A.O. Leu, S.J. McIlroy, J. Ye, D.H. Parks, V.J. Orphan, G.W. Tyson, Lateral Gene Transfer Drives Metabolic Flexibility in the Anaerobic Methane-Oxidizing Archaeal Family *Methanoperedenaceae*, mBio 11 (2020) e01325-01320.

[15] K.F. Ettwig, B.L. Zhu, D. Speth, J.T. Keltjens, M.S.M. Jetten, B. Kartal, Archaea catalyze iron-dependent anaerobic oxidation of methane, P Natl Acad Sci USA 113 (2016) 12792-12796.

[16] A. Arshad, D.R. Speth, R.M. de Graaf, H.J. Op den Camp, M.S. Jetten, C.U. Welte, A Metagenomics-Based Metabolic Model of Nitrate-Dependent Anaerobic Oxidation of Methane by Methanoperedens-Like Archaea, Front Microbiol 6 (2015) 1423.

[17] W.B. Liu, H.W. Xiao, H.P. Ma, Y.Y. Li, T.M. Adyel, J. Zhai, Reduction of methane emissions from manganese-rich constructed wetlands: Role of manganese-dependent anaerobic methane oxidation, Chemical Engineering Journal 387 (2020) 123402.

[18] J. Ding, Z.W. Ding, L. Fu, Y.Z. Lu, S.H. Cheng, R.J. Zeng, New primers for detecting and quantifying denitrifying anaerobic methane oxidation archaea in different ecological niches, Appl Microbiol Biot 99 (2015) 9805-9812.

[19] Y. Peng, H.C.M. Leung, S.M. Yiu, F.Y.L. Chin, IDBA-UD: a de novo assembler for single-cell and metagenomic sequencing data with highly uneven depth, Bioinformatics 28 (2012) 1420-1428.

[20] D.D. Kang, J. Froula, R. Egan, Z. Wang, MetaBAT, an efficient tool for accurately reconstructing single genomes from complex microbial communities, Peerj 3 (2015) e1165.

[21] M.R. Olm, C.T. Brown, B. Brooks, J.F. Banfield, dRep: a tool for fast and accurate genomic comparisons that enables improved genome recovery from metagenomes through de-replication, Isme J 11 (2017) 2864-2868.

[22] D.H. Parks, M. Imelfort, C.T. Skennerton, P. Hugenholtz, G.W. Tyson, CheckM: assessing the quality of microbial genomes recovered from isolates, single cells, and metagenomes, Genome Res 25 (2015) 1043-1055.

[23] K.F. Ettwig, S. Shima, K.T. van de Pas-Schoonen, J. Kahnt, M.H. Medema, H.J.M. op den Camp, M.S.M. Jetten, M. Strous, Denitrifying bacteria anaerobically oxidize methane in the absence of Archaea, Environ Microbiol 10 (2008) 3164-3173.

[24] C.J. Schubert, F. Vazquez, T. Losekann-Behrens, K. Knittel, M. Tonolla, A. Boetius, Evidence for anaerobic oxidation of methane in sediments of a freshwater system (Lago di Cadagno), Fems Microbiol Ecol 76 (2011) 26-38.

[25] G. Wegener, V. Krukenberg, D. Riedel, H.E. Tegetmeyer, A. Boetius, Intercellular wiring enables electron transfer between methanotrophic archaea and bacteria, Nature 526 (2015) 587-U315.

[26] A. Vaksmaa, M.S.M. Jetten, K.F. Ettwig, C. Luke, *McrA* primers for the detection

and quantification of the anaerobic archaeal methanotroph '*Candidatus* Methanoperedens nitroreducens', Appl Microbiol Biot 101 (2017) 1631-1641.

[27] D. Liu, Y. Yang, J. Ai, Y. Li, Y. Xing, J. Li, Research on microbial structures, functions and metabolic pathways in an advanced denitrification system coupled with aerobic methane oxidation based on metagenomics, Bioresource Technology 332 (2021).

[28] T.J. Lawton, A.C. Rosenzweig, Methane-Oxidizing Enzymes: An Upstream Problem in Biological Gas-to-Liquids Conversion, J Am Chem Soc 138 (2016) 9327-9340.

[29] R.O. Thiago, B. Aline, V. Deborah, S. Bernhard, C.M. Kyaw, Archaeal S-Layers: Overview and Current State of the Art, Front Microbiol 08 (2017) 2597.

[30] L. Shi, K.M. Rosso, T.A. Clarke, D.J. Richardson, J.M. Zachara, J.K. Fredrickson, Molecular Underpinnings of Fe(III) Oxide Reduction by Shewanella Oneidensis MR-1, Front Microbiol 3 (2012) 50.

[31] S. Vieira, M. Luckner, G. Wanner, J. Overmann, Luteitalea pratensis gen. nov., sp. nov. a new member of subdivision 6 Acidobacteria isolated from temperate grassland soil, Int J Syst Evol Micr 67 (2017) 1408-1414.

[32] H. Lin, N.H. Szeinbaum, T.J. DiChristina, M. Taillefert, Microbial Mn(IV) reduction requires an initial one-electron reductive solubilization step, Geochim Cosmochim Ac 99 (2012) 179-192.

[33] A. Qian, W. Zhang, C. Shi, C. Pan, D.E. Giammar, S. Yuan, H. Zhang, Z. Wang, Geochemical Stability of Dissolved Mn(III) in the Presence of Pyrophosphate as a Model Ligand: Complexation and Disproportionation, Environ Sci Technol 53 (2019) 5768-5777.

[34] G. Su, J. Zopfi, H. Yao, L. Steinle, H. Niemann, M.F. Lehmann, Manganese/iron-supported sulfate-dependent anaerobic oxidation of methane by archaea in lake sediments, Limnol Oceanogr 65 (2020) 863-875.

[35] L. Gao, X. Lu, H. Liu, J. Li, W. Li, R. Song, R. Wang, D. Zhang, J. Zhu, Mediation of extracellular polymeric substances in microbial reduction of hematite by shewanella oneidensismr-1, Front Microbiol 10 (2019).

[36] L. Shi, H.L. Dong, G. Reguera, H. Beyenal, A.H. Lu, J. Liu, H.Q. Yu, J.K. Fredrickson, Extracellular electron transfer mechanisms between microorganisms and minerals, Nat Rev Microbiol 14 (2016) 651-662.

[37] M.J. Edwards, G.F. White, J.N. Butt, D.J. Richardson, T.A. Clarke, The Crystal Structure of a Biological Insulated Transmembrane Molecular Wire, Cell 181 (2020) 665-673.e610.

[38] Y. Gu, V. Srikanth, A.I. Salazar-Morales, R. Jain, J.P. O'Brien, S.M. Yi, R.K. Soni, F.A. Samatey, S.E. Yalcin, N.S. Malvankar, Structure of *Geobacter* pili reveals secretory rather than nanowire behaviour, Nature 597 (2021) 430-434.

Declaration of interests

☒ The authors declare that they have no known competing financial interests or personal relationships that could have appeared to influence the work reported in this paper.

☐ The authors declare the following financial interests/personal relationships which may be considered as potential competing interests:

Highlights

- Anaerobic consortia mediate Mn-dependent AOM via syntrophic pathway
- *Ca. Methanoperedens* sp. BLZ1 mediates CH_4 oxidation via reverse methanogenesis
- Interspecies electron transfer is by conductive pili of *Luteitalea pratensis*
- *Luteitalea pratensis* perform Mn(IV) reduction via multi-heme c-type cytochrome

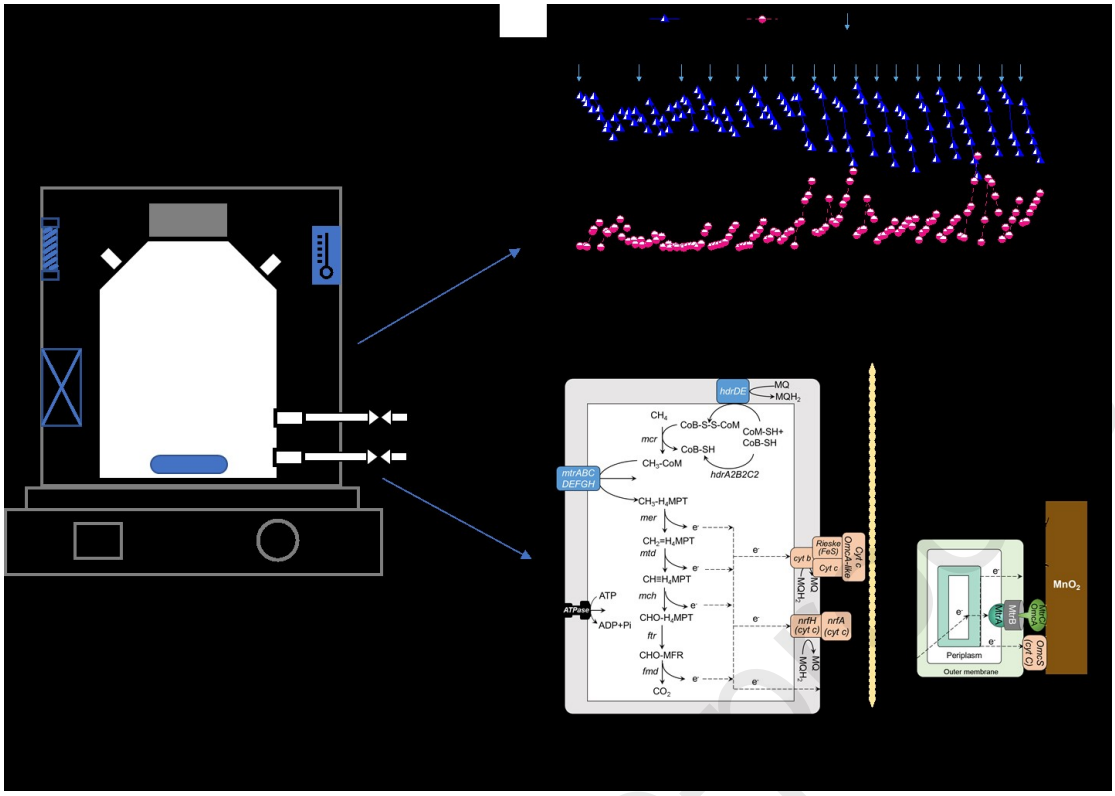

444